Beauty of Wear

Vahid.Javaheri@oulu.fi

UNIVERSITY OF OULU

CASR Centre for Advanced Steels Research

Wear 496–497 (2022) 204301

Contents lists available at ScienceDirect

Wear

journal homepage: www.elsevier.com/locate/wear

Check for updates

Formation of nanostructured surface layer, the white layer, through solid particles impingement during slurry erosion in a martensitic medium-carbon steel

V. Javaheri [a,*], S. Sadeghpour [a], P. Karjalainen [a], M. Lindroos [b], O. Haiko [a], N. Sarmadi [c], S. Pallaspuro [a], K. Valtonen [d], F. Pahlevani [c], A. Laukkanen [b], J. Kömi [a]

[a] *Materials and Mechanical Engineering, Centre for Advanced Steels Research, University of Oulu, Finland*
[b] *Integrated Computational Materials Engineering, VTT Technical Research Centre of Finland, Espoo, Finland*
[c] *Centre for Sustainable Materials Research and Technology, SMaRT@UNSW, School of Materials Science and Engineering, UNSW, Sydney, Australia*
[d] *Tampere Wear Center, Materials Science and Environmental Engineering, Faculty of Engineering and Natural Sciences, Tampere University, Finland*

A R T I C L E I N F O

Keywords:
White layer
Martensitic steel
Slurry erosion
Nanocrystalline structure
Cell formation
Martensite deformation
Nanohardness

A B S T R A C T

The extremely altered topmost surface layer, known as the white layer, formed in a medium-carbon low-alloy steel as result of impacts by angular 10–12 mm granite particles during the slurry erosion process is comprehensively investigated. For this purpose, the characteristics, morphology, and formation mechanism of this white layer are described based on the microstructural observations using optical, scanning and transmission electron microscopies as well as nanoindentation hardness measurements and modelling of surface deformation. The white layer exhibits a nanocrystalline structure consisting of ultrafine grains with an average size of 200 nm. It has a nanohardness level of around 10.1 GPa, considerably higher than that of untempered martensitic bulk material (5.7 GPa) achieved by an induction hardening treatment. The results showed that during the high-speed slurry erosion process, solid particle impacts brought forth conditions of high strain, high strain rate, and multi-directional strain paths. This promoted formation of a cell-type structure at first and later, after increasing the number of impacts, development of subgrains following by subgrain rotation and eventually formation of a nanocrystalline structure with ultra-high hardness. The model confirmed that high strain conditions - much higher than required for the onset of plastic deformation - can be achieved on the surface resulting in severe microstructural and property changes during the slurry erosion test.

Science with Arctic Attitude

University of Oulu

#unioulu #arcticattitude

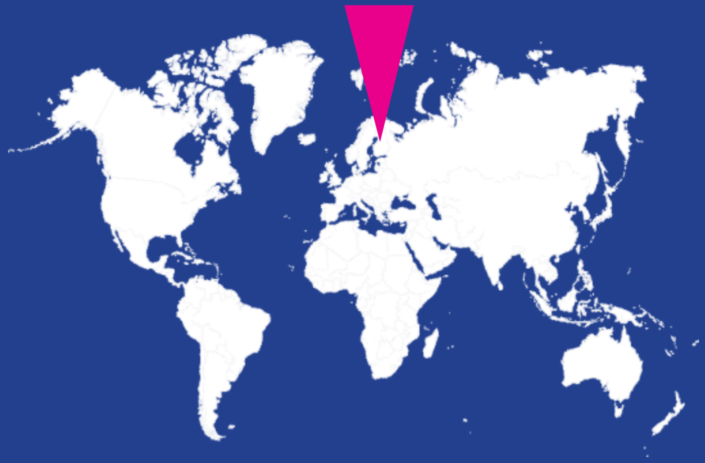

University of Oulu founded

1958

Multidisciplinary research and education

- Natural Sciences and Mathematics
- Biosciences
- Medicine and Health
- Economics and Business Administration
- Engineering and Architecture
- Information and Communication Technologies
- Education
- Humanities

50 000+
Alumni

13 800
Students

3 700
Staff

Materials and Mechanical Engineering Unit

Microstructure & Mechanics	Ultrahigh-Strength Steel	Modelling	Fatigue
Corrosion	Machine Design	Education	

>4 M€
Budget

94 (150)
Publications 2020 (2021)

74
Staff

Material & Methods

- The material used in this work (designed by the authors) was a new medium-carbon, low alloy steel microalloyed with Nb with the following composition: **0.4C-0.2Si-0.25Mn-0.90Cr-0.50Mo** and **0.013Nb (wt. %).**

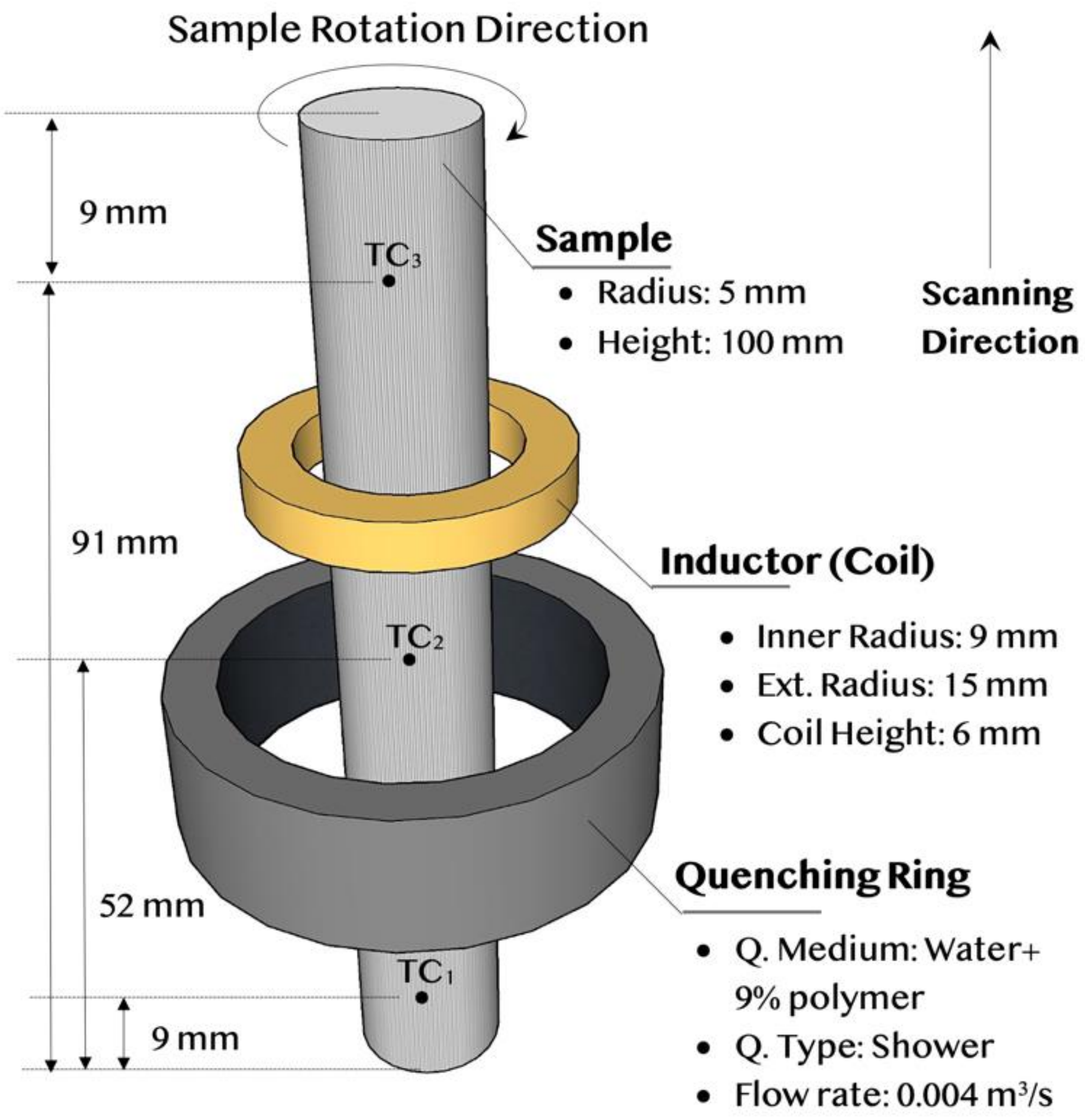

High-speed slurry-pot

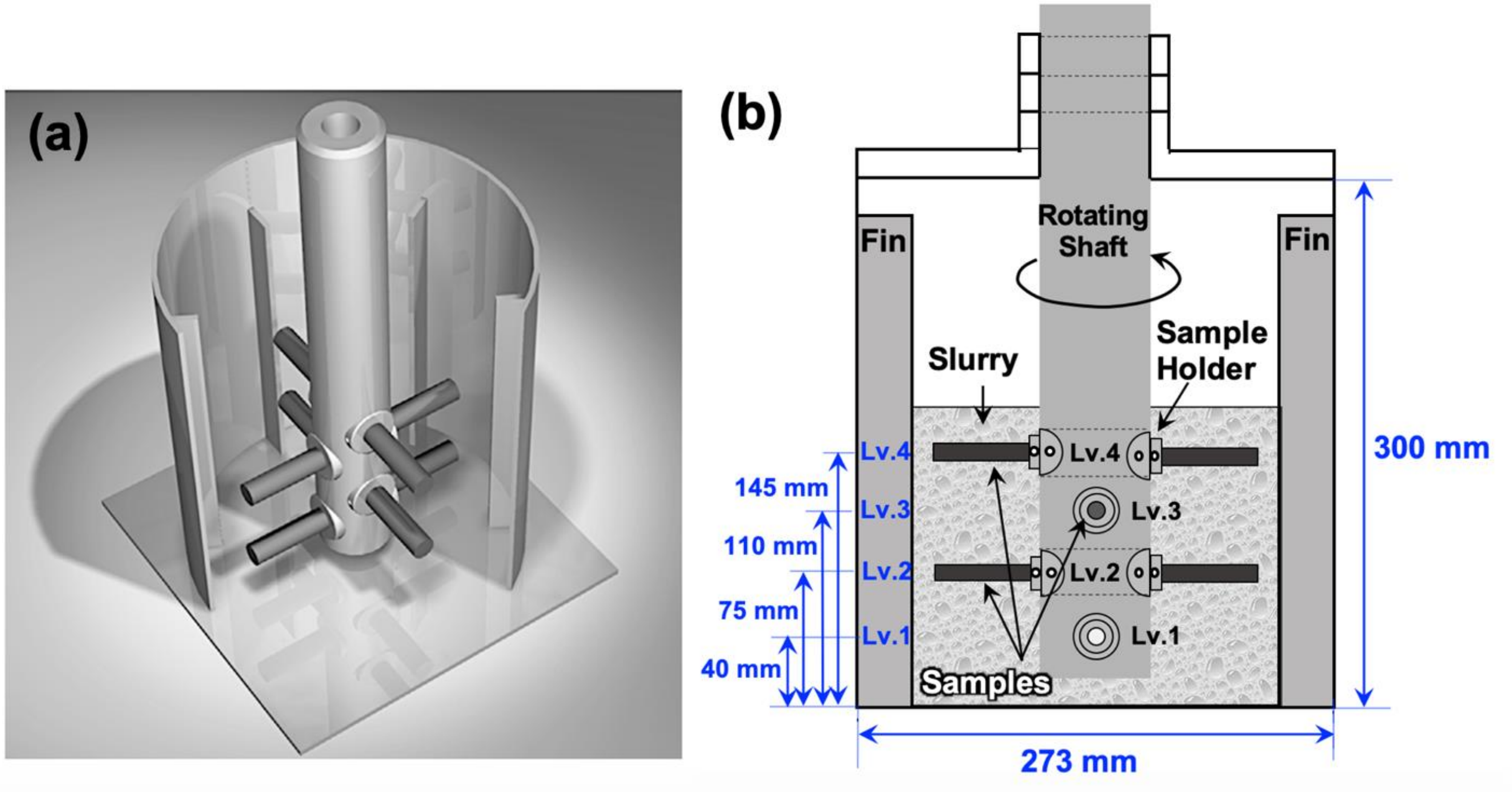

High-speed slurry-pot

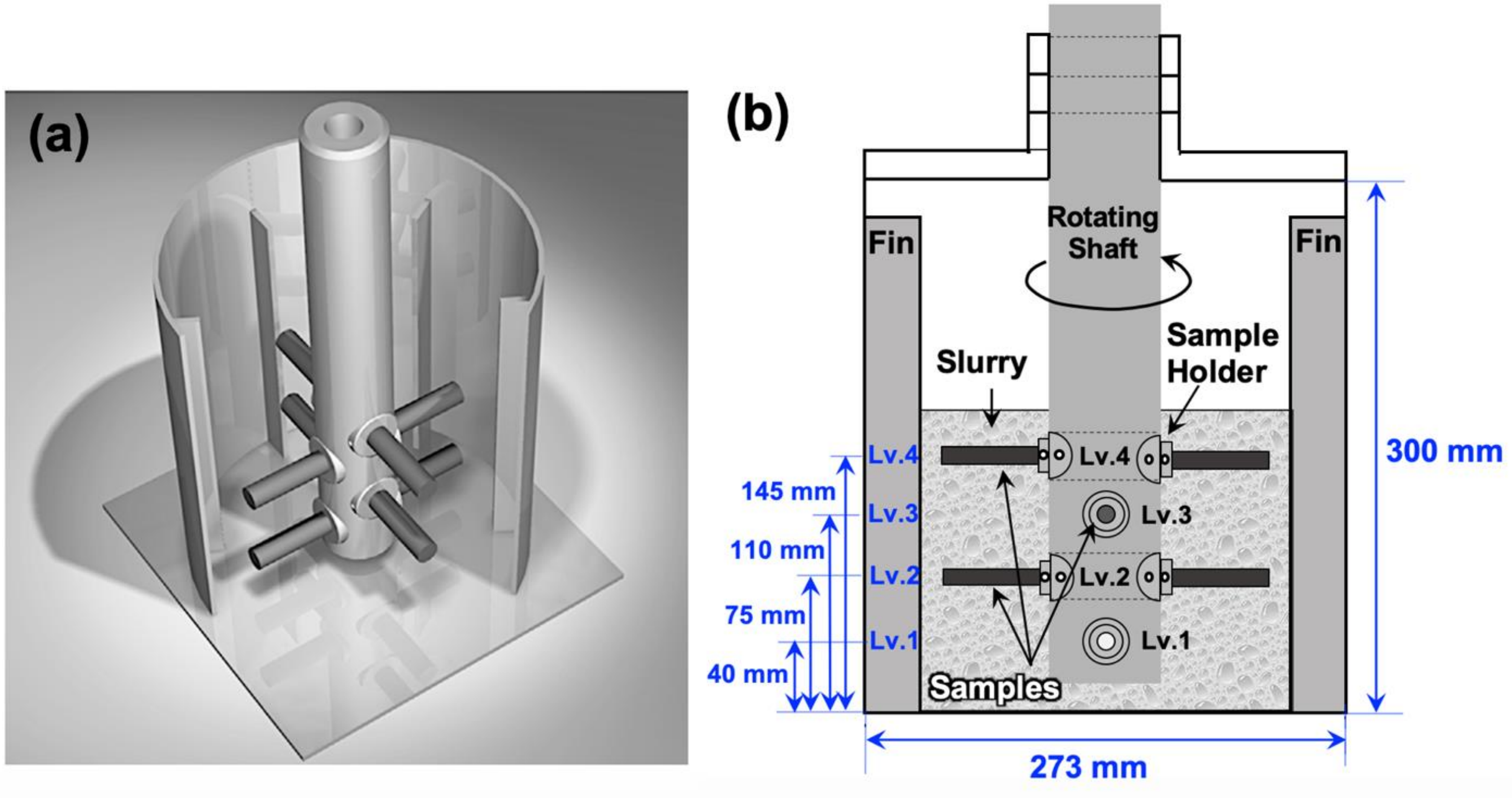

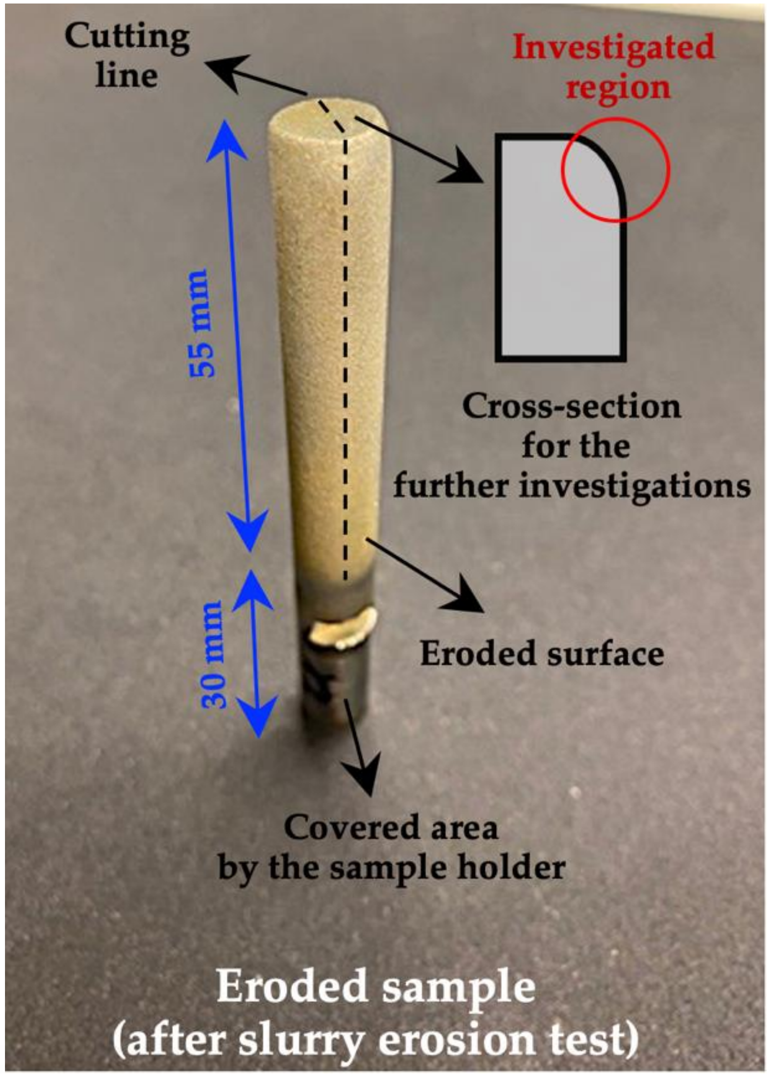

On the role of grain size on slurry erosion behavior of a novel medium-carbon, low- alloy pipeline steel after induction hardening.
V Javaheri, O Haiko, S Sadeghpour, K Valtonen, J Kömi, D Porter. Wear, 203678.

Microstructure

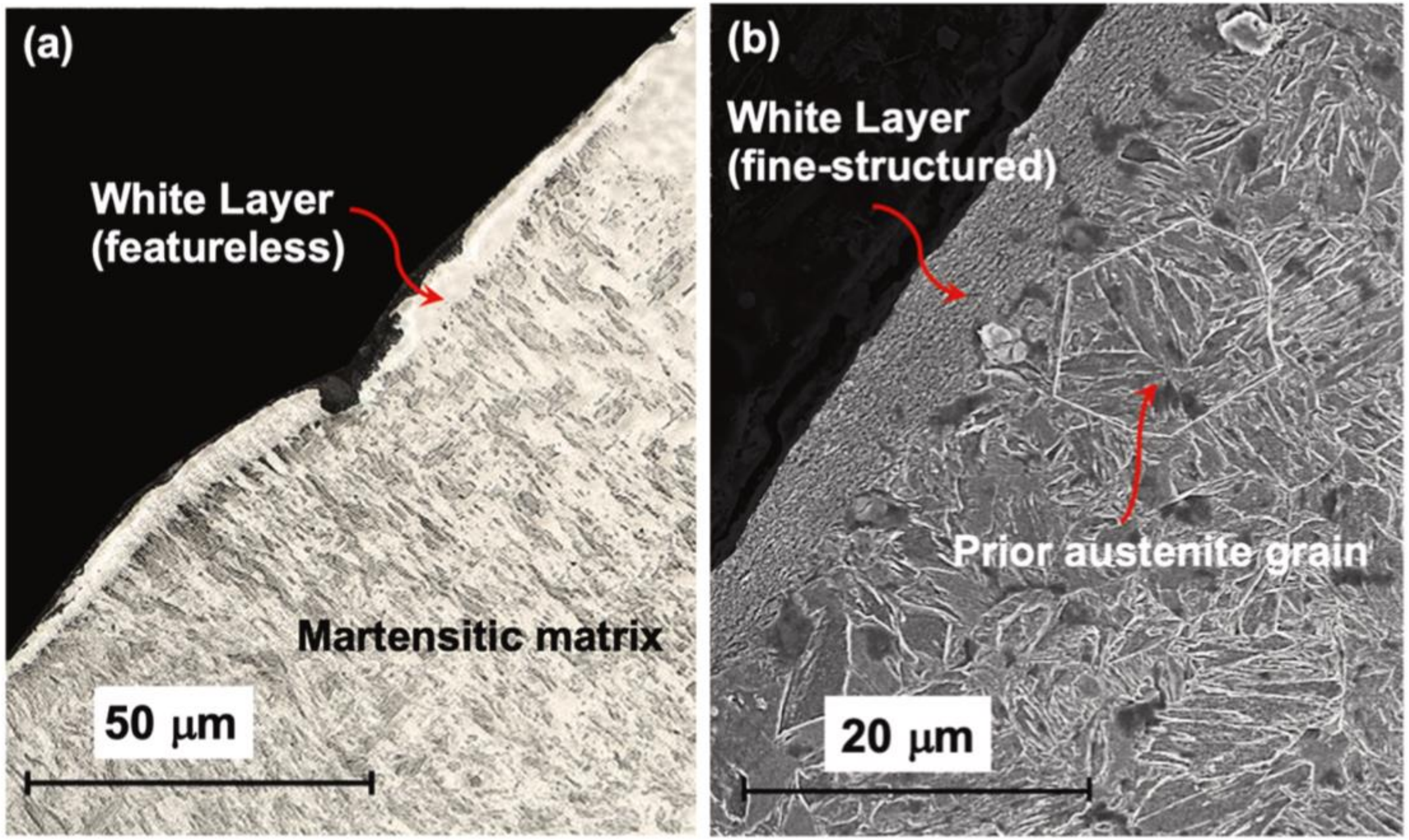

Fig. 4. a) Combined optical and laser scanning confocal image and b) SEM micrograph of the eroded surface (cross-section) indicating the formation of a superficial white layer on the top of the eroded surface and the martensitic microstructure of the bulk material.

Microstructure

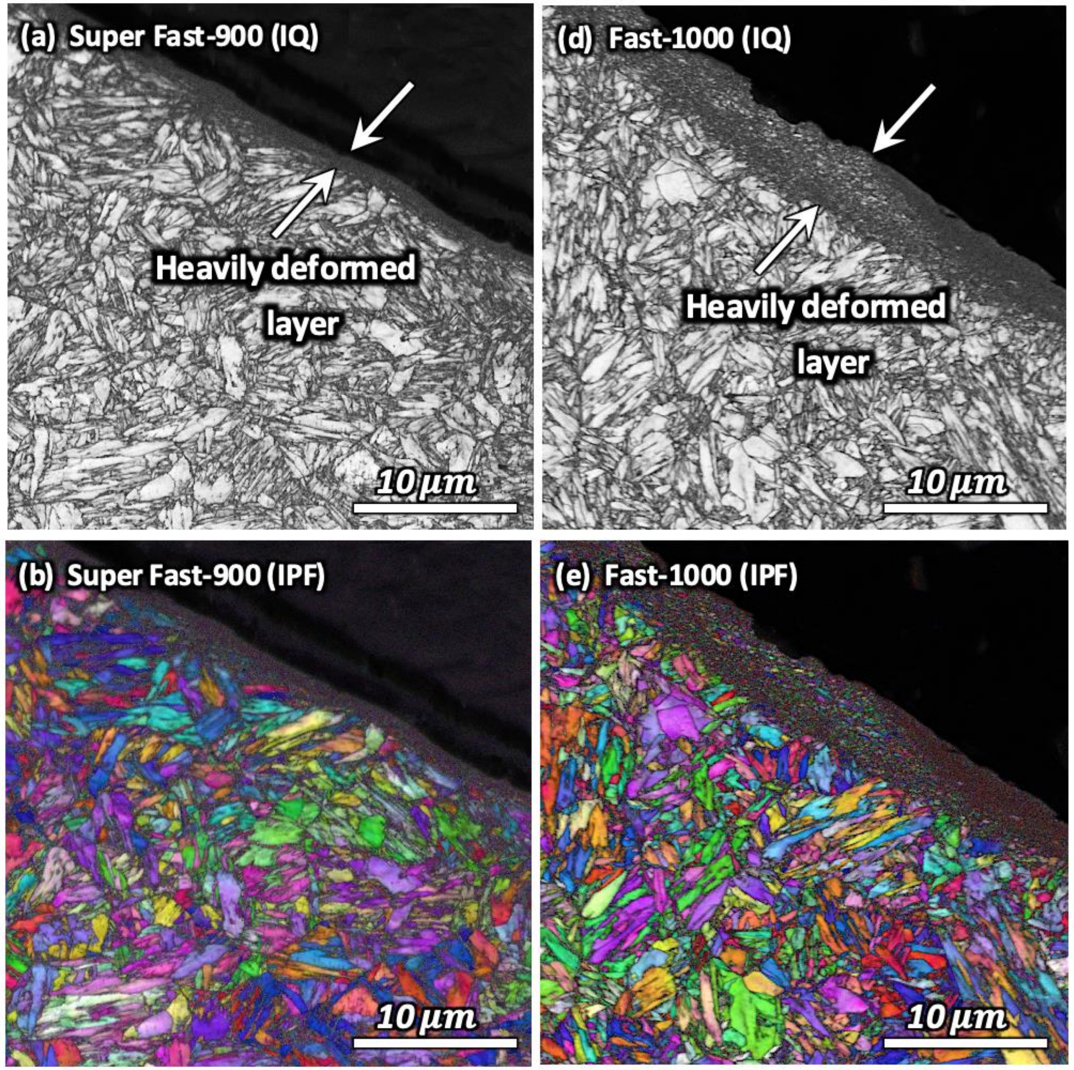

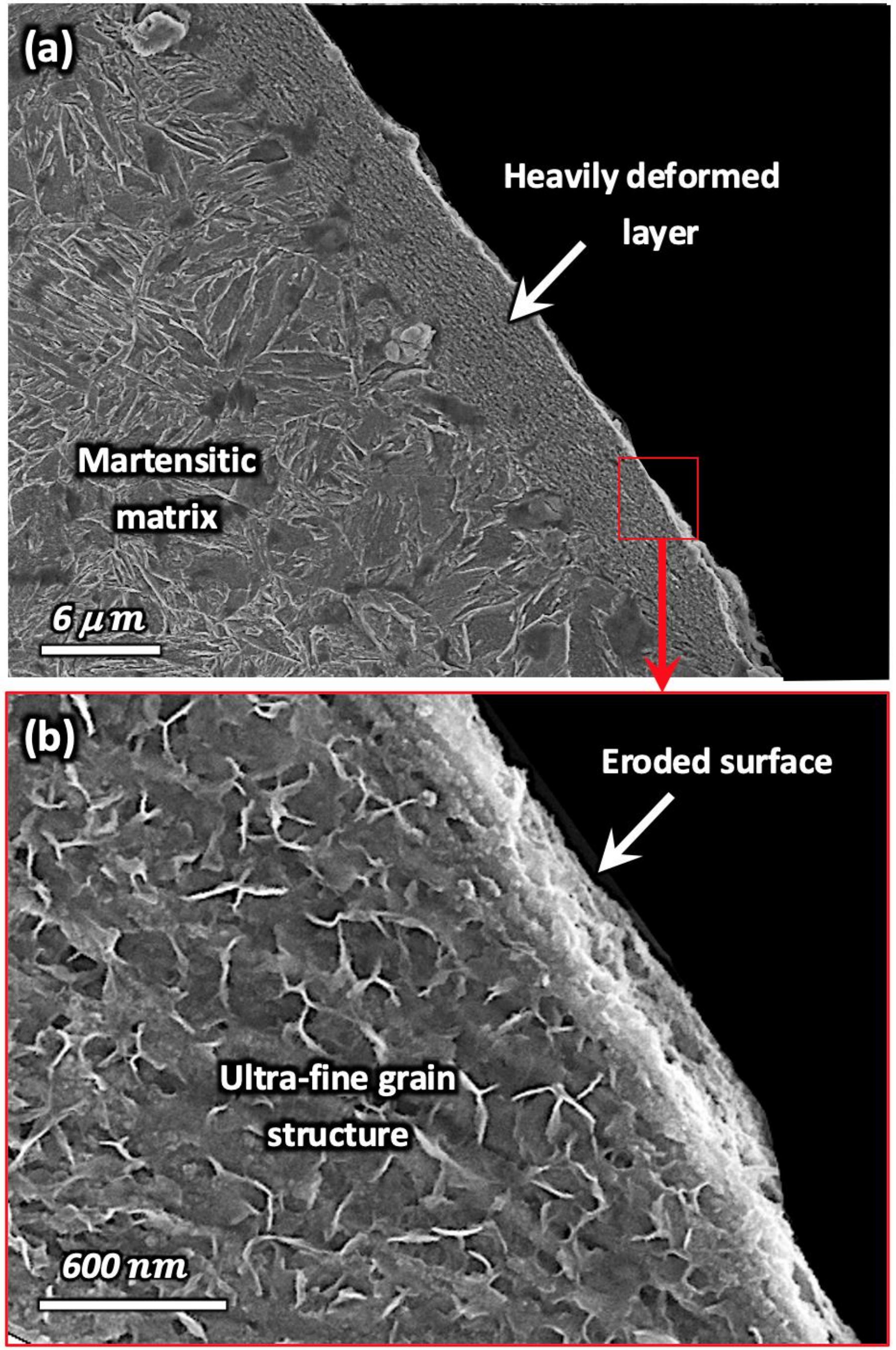

TEM Dark Field vs EBSD

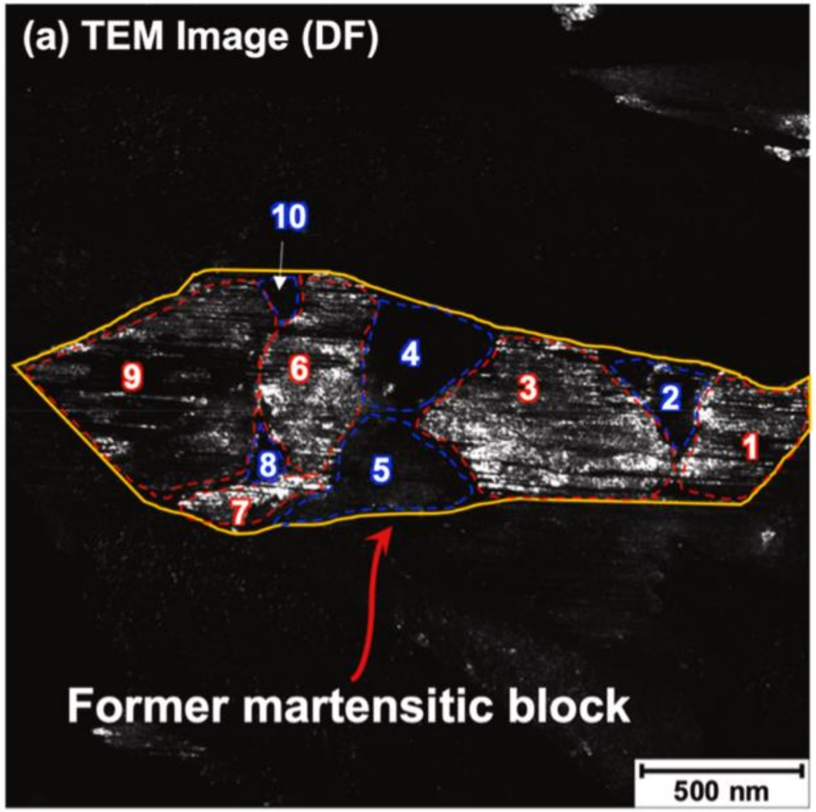

Fig. 7. Formation of dislocation cells inside the prior martensite block obtained from a) TEM dark field image (The cells with almost the same orientation have been numbered with the same color) and b) EBSD inverse pole figure maps of two neighbor blocks. (For interpretation of the references to color in this figure legend, the reader is referred to the Web version of this article.)

FIB Samples

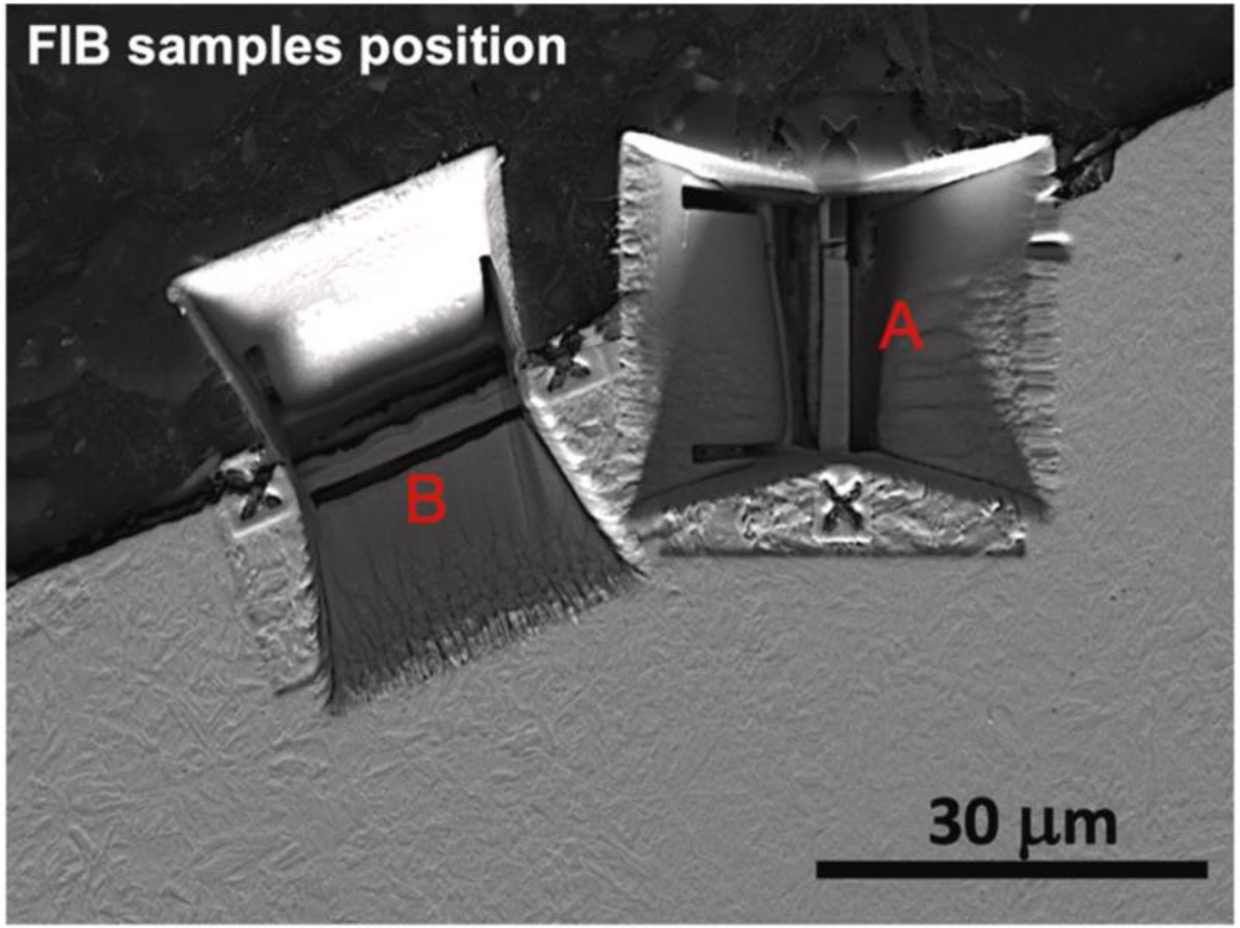

Fig. 2. The position of TEM foils prepared by FIB technique from the regions that contain the bulk material and white layer (A) and only the white layer (B).

Sample A

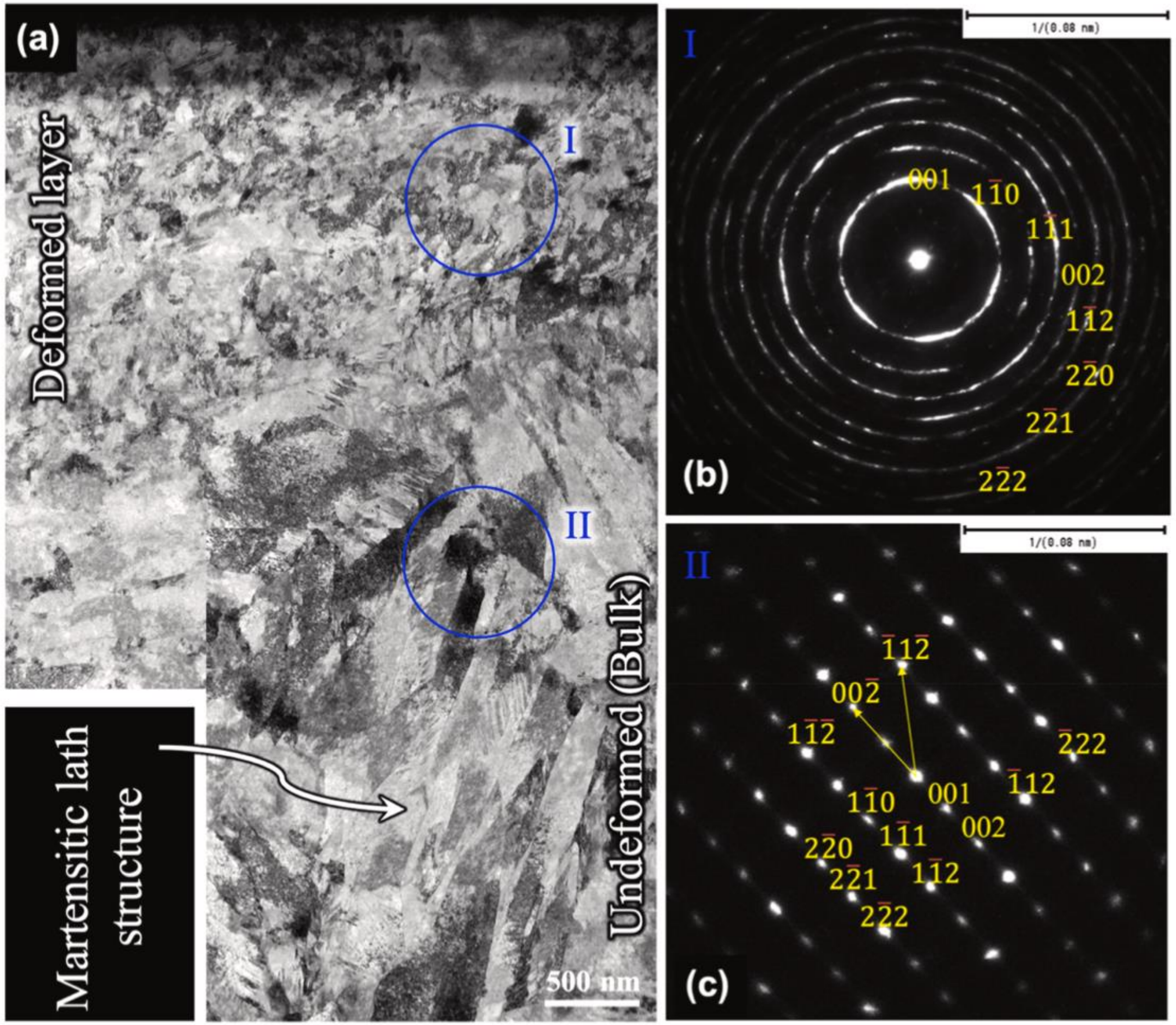

Fig. 5. a) STEM micrographs along with b-c) the corresponding selected area diffraction patterns (SADPs), acquired from the FIB sample A and viewed from the [110] zone axis. b) SADP for the white layer highlighted as region I in Fig. 5(a) and b) SADP for the bulk material highlighted as region II in Fig. 5(a). To cover a larger area and provide sufficient information two STEM images are stitched together in Fig. 5(a).

5

Sample B

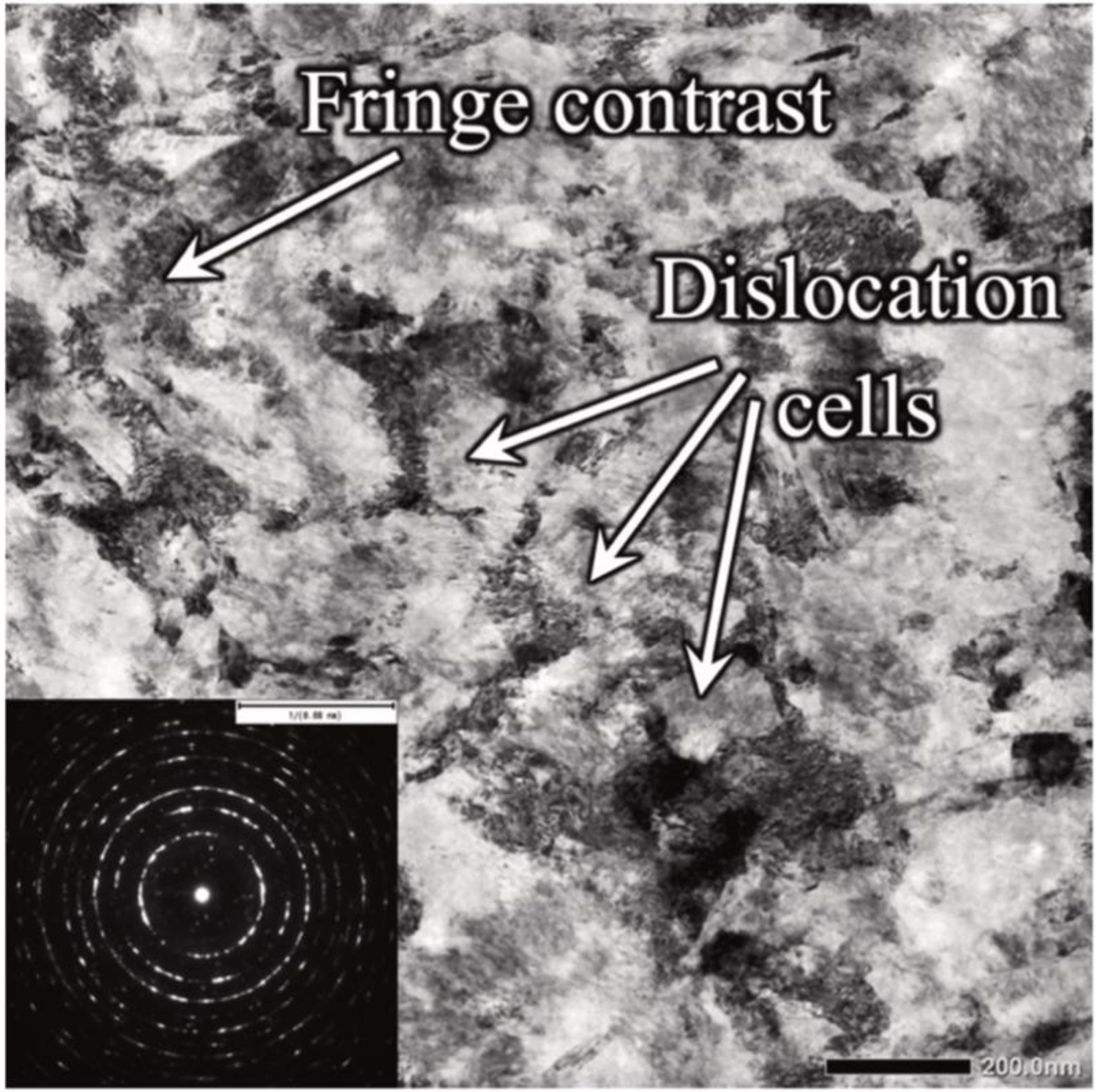

Fig. 6. STEM micrograph of the WL (sample B) and the corresponding SADP showing the dislocation cell-type structure.

Modelling

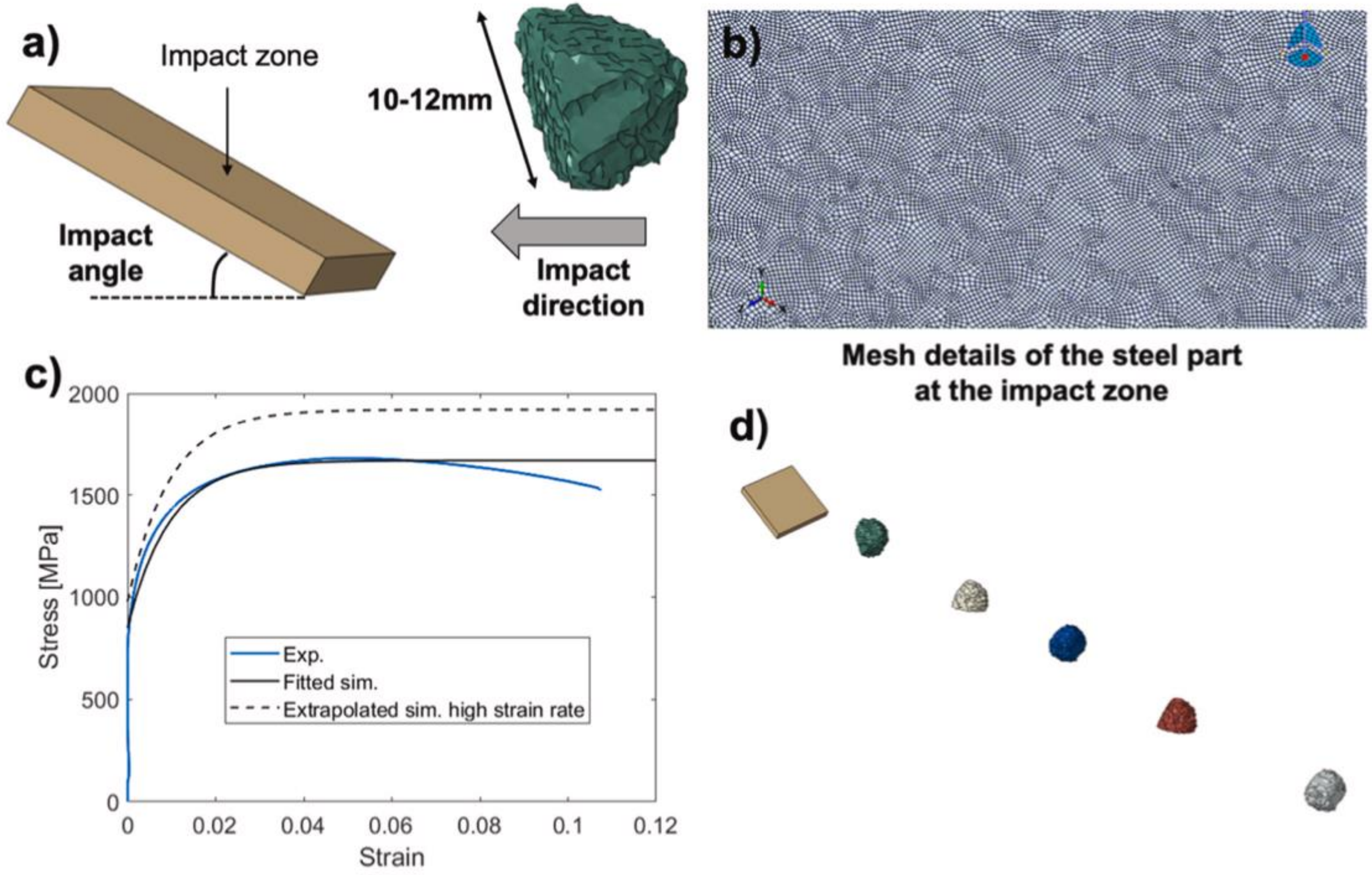

Fig. 3. a) The oblique-angle impact model assembly with rough rocks impacting steel surface, b) mesh details for the analyzed steel part, c) stress-strain behavior for the elasto-plastic model with low strain rate condition (0.008 s^{-1}) and extrapolated high strain rate behavior (4000 s^{-1}), d) five rocks impact assembly.

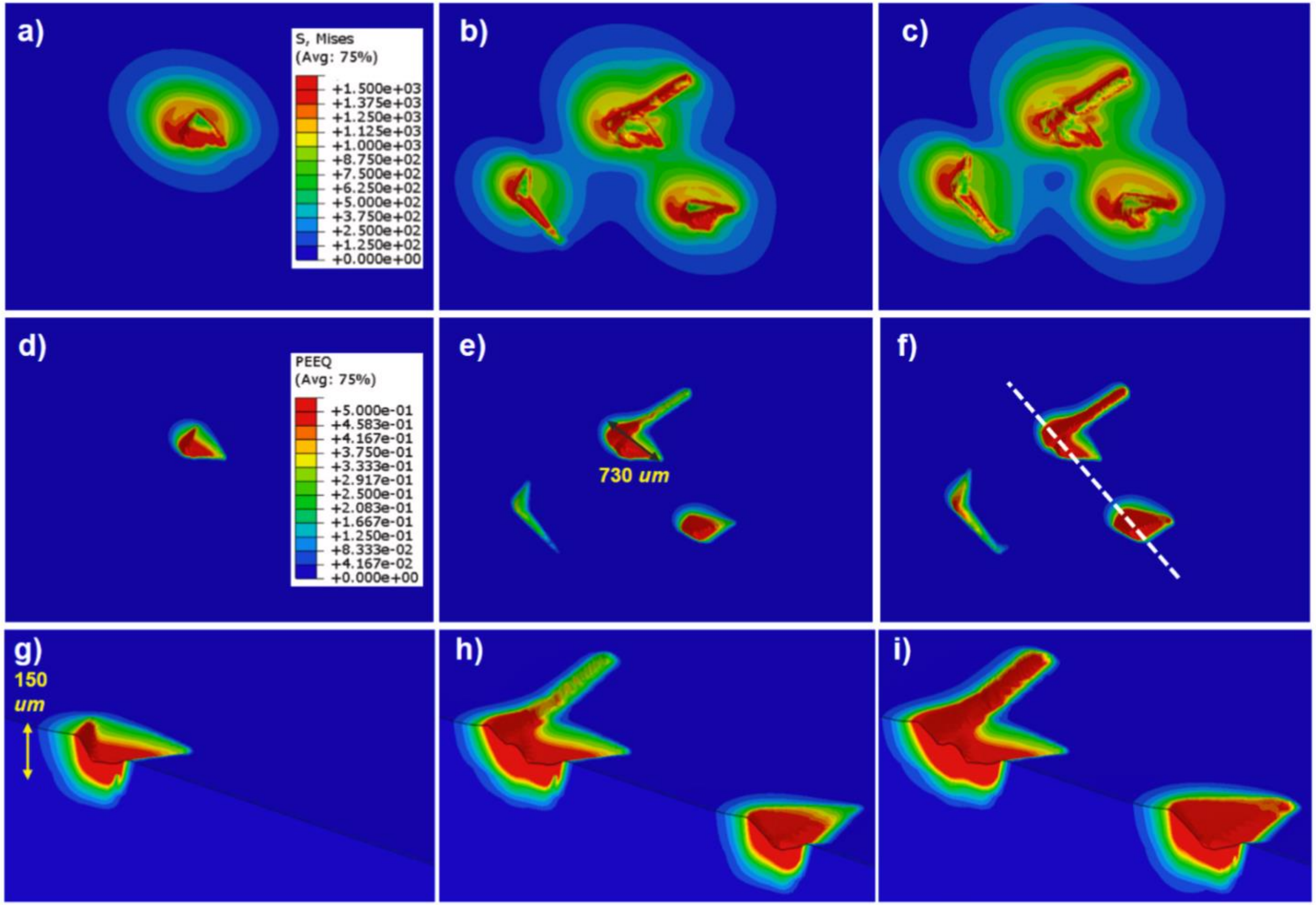

Fig. 11. Von Mises stress (a–c) and equivalent plastic strain distribution (d–i) after a single impact, three impacts, five impacts. Cross-section, shown in (g–i), is marked with a white dashed line on f) and the impact angle is 30°.

Equivalent Plastic Strain

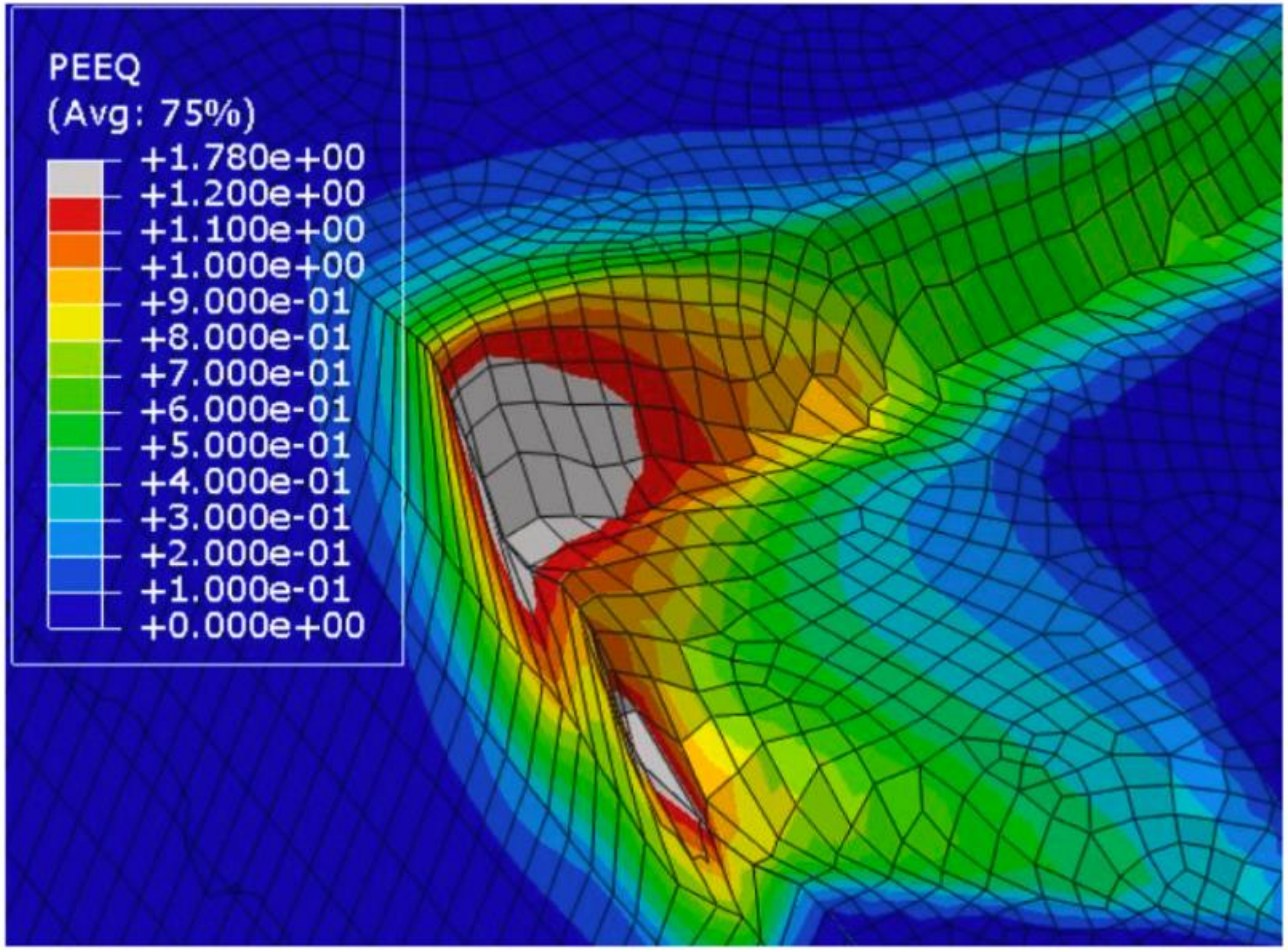

Fig. 12. The maximum equivalent plastic strain on the topmost surface region after five impacts.

Surface Damage

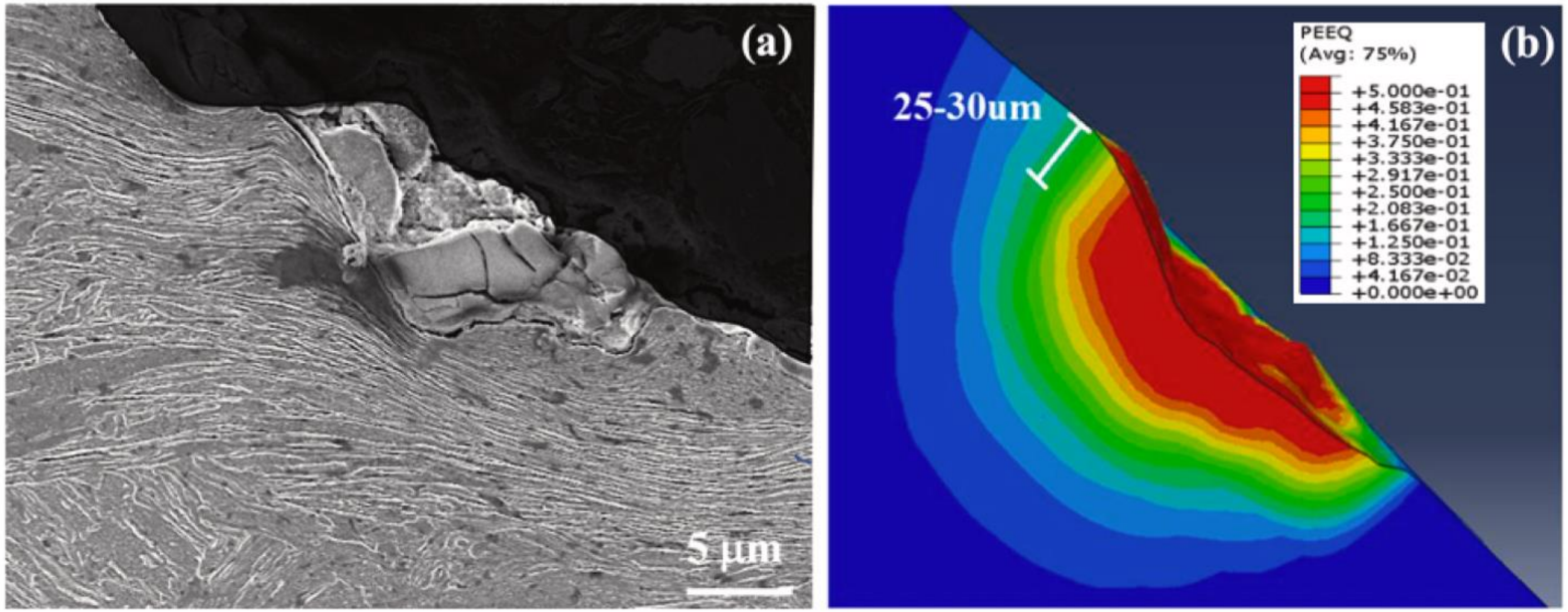

Fig. 13. Two examples of extensive strain and plastic flow as a results of particle impact on the surface. A) SEM image of a cross-sectioned eroded surface and b) a modeling result.

Mechanism

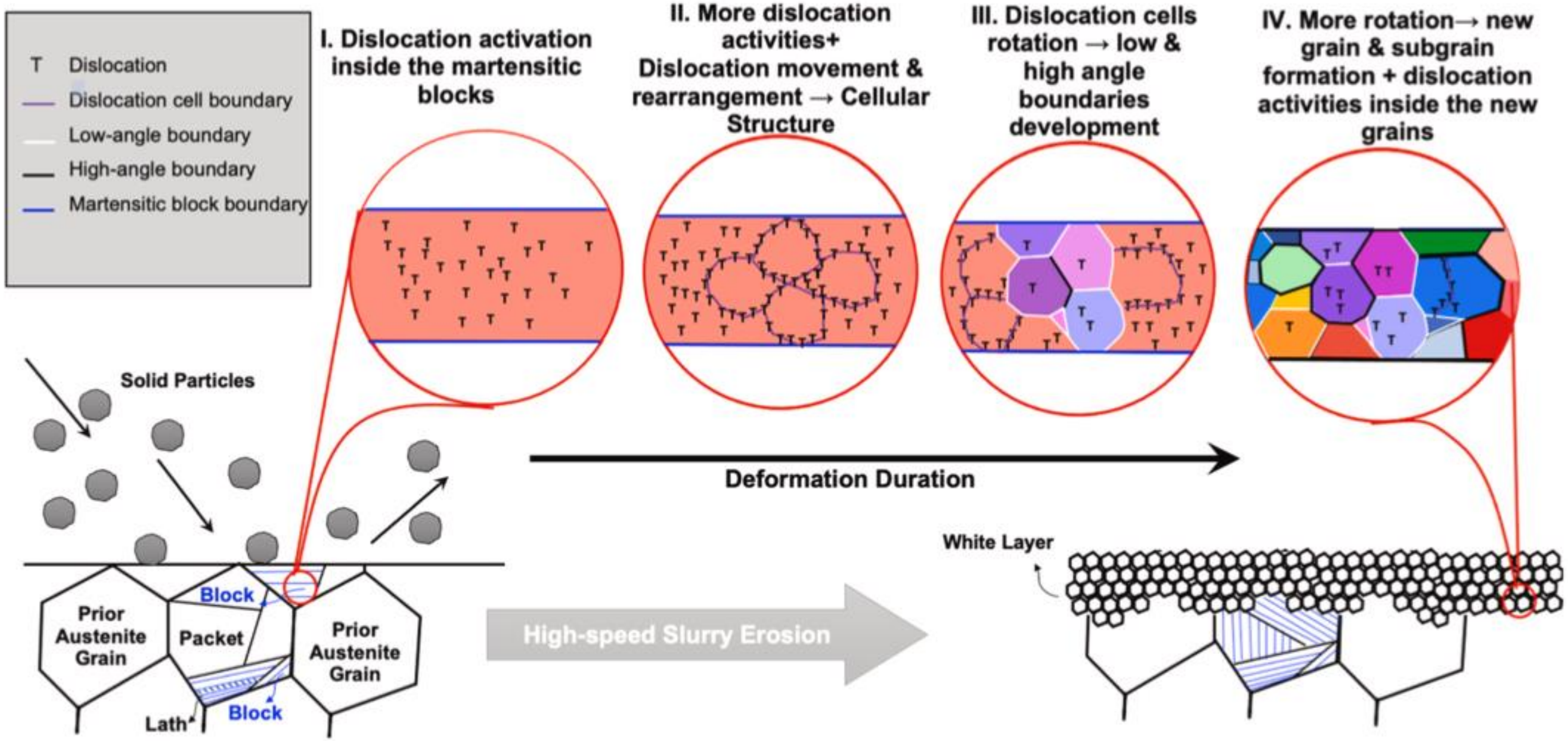

Fig. 10. An illustration for the mechanism of formation of nanocrystalline structure in WL because of the solid particle impacts during the slurry erosion process.


SO WHAT?

Nanohardness

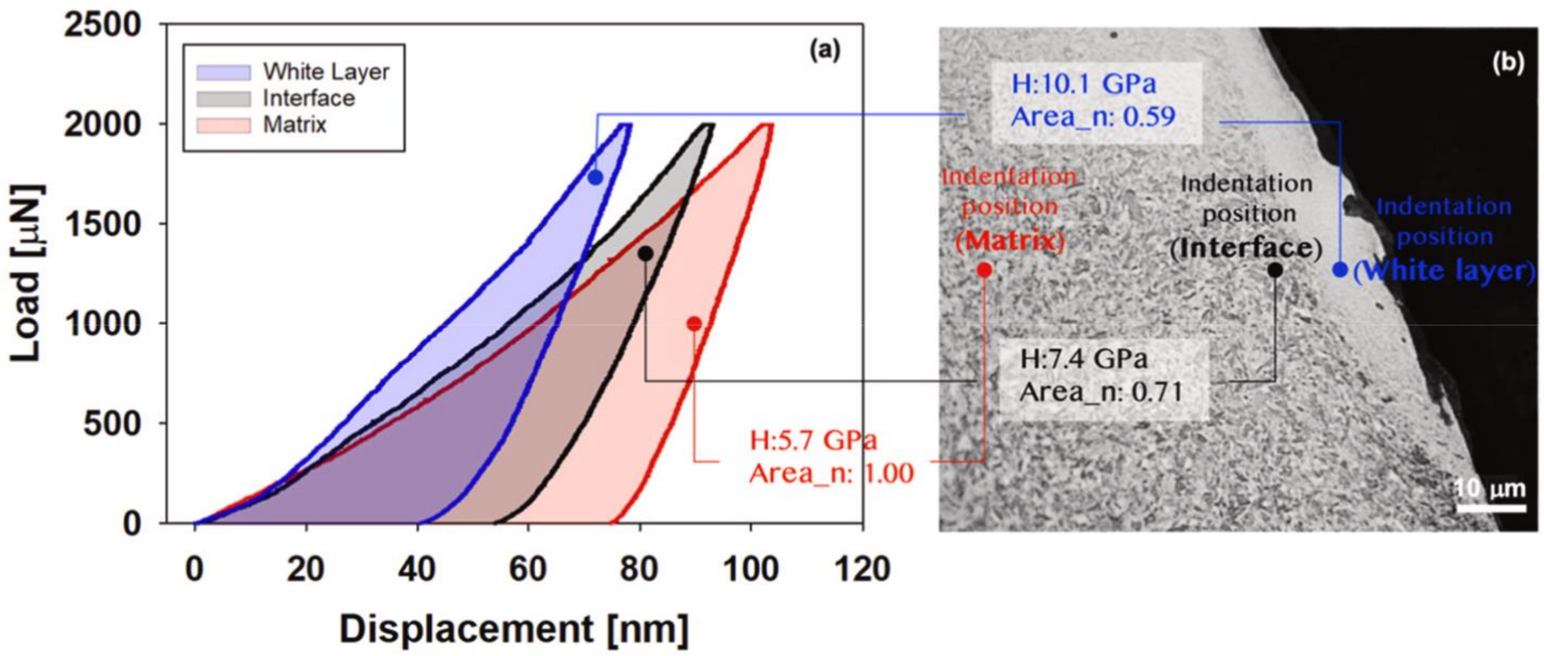

Fig. 14. a) The displacement-load curves of WL, bulk material, and interface region along with b) the hardness value, the ratio of area under each curve to the area under bulk material curve (Area _n) and position of each measurement.

Nanohardness

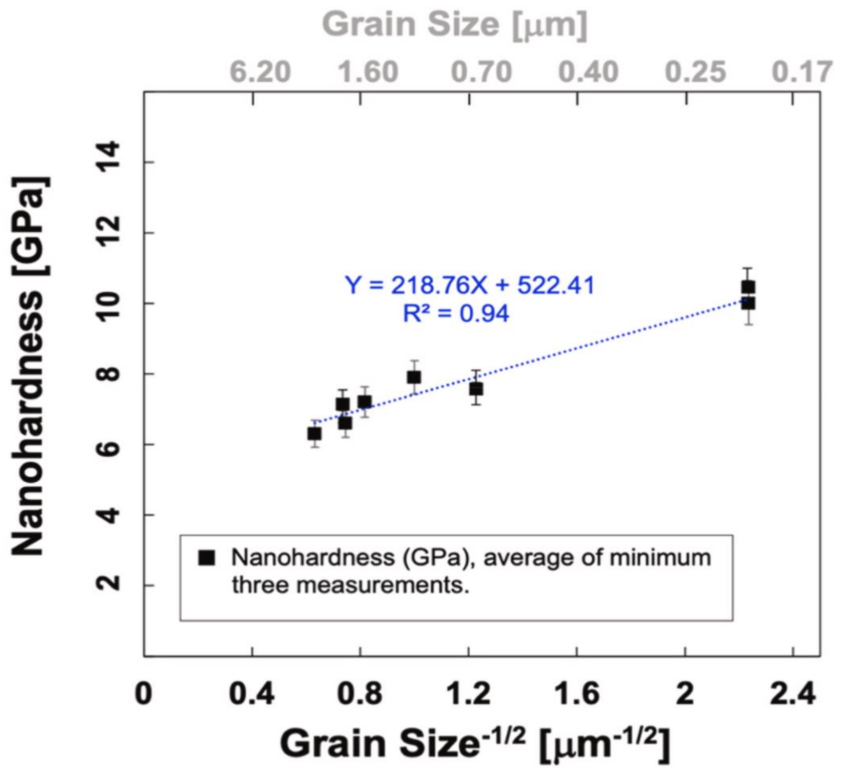

Fig. 15. The relation between the grain size and hardness indicating a typical Hall-Petch behavior.

Nanohardness

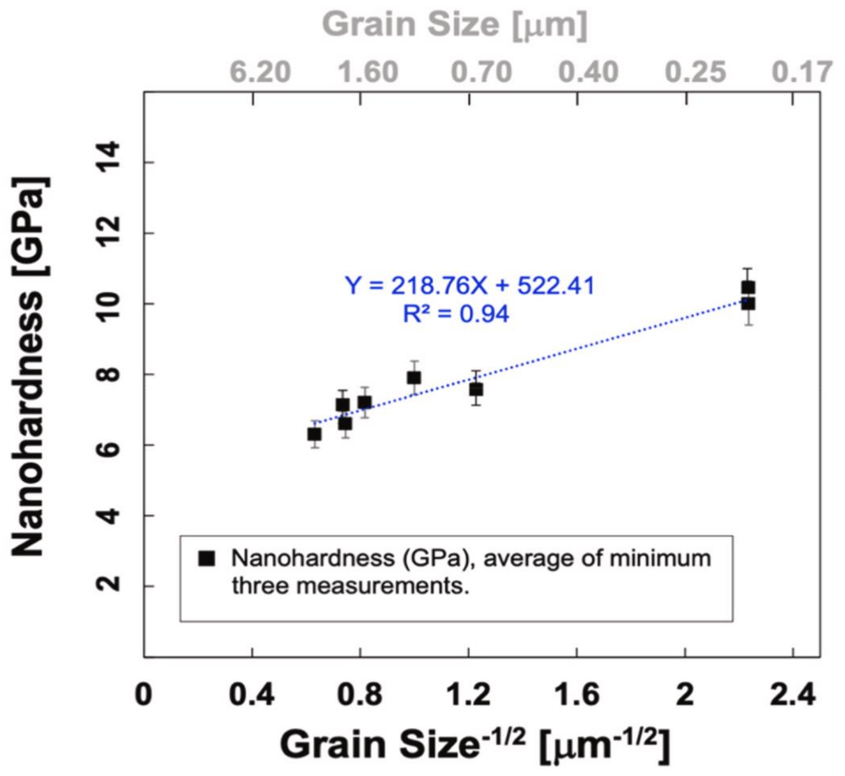

Fig. 15. The relation between the grain size and hardness indicating a typical Hall-Petch behavior.

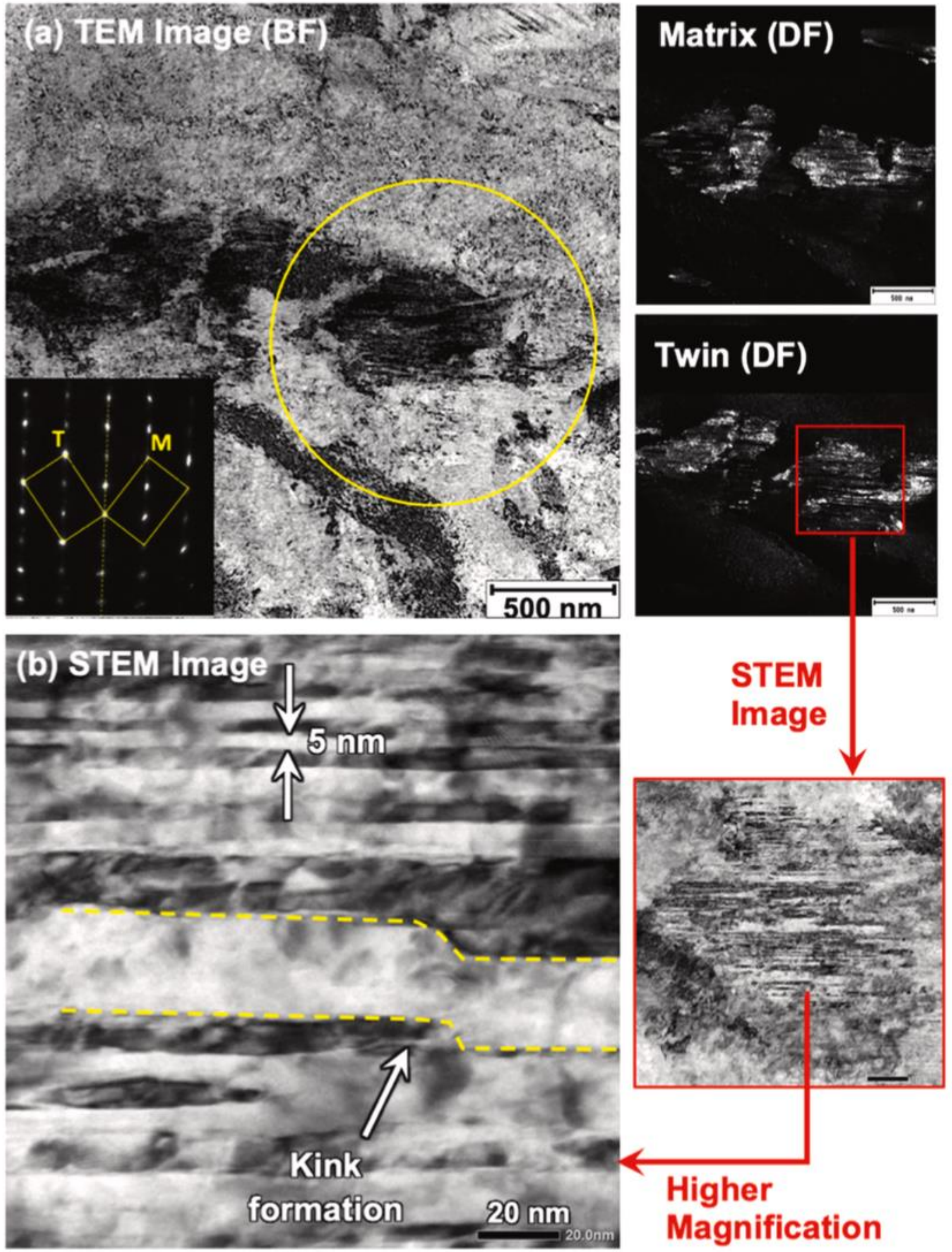

Nanohardness

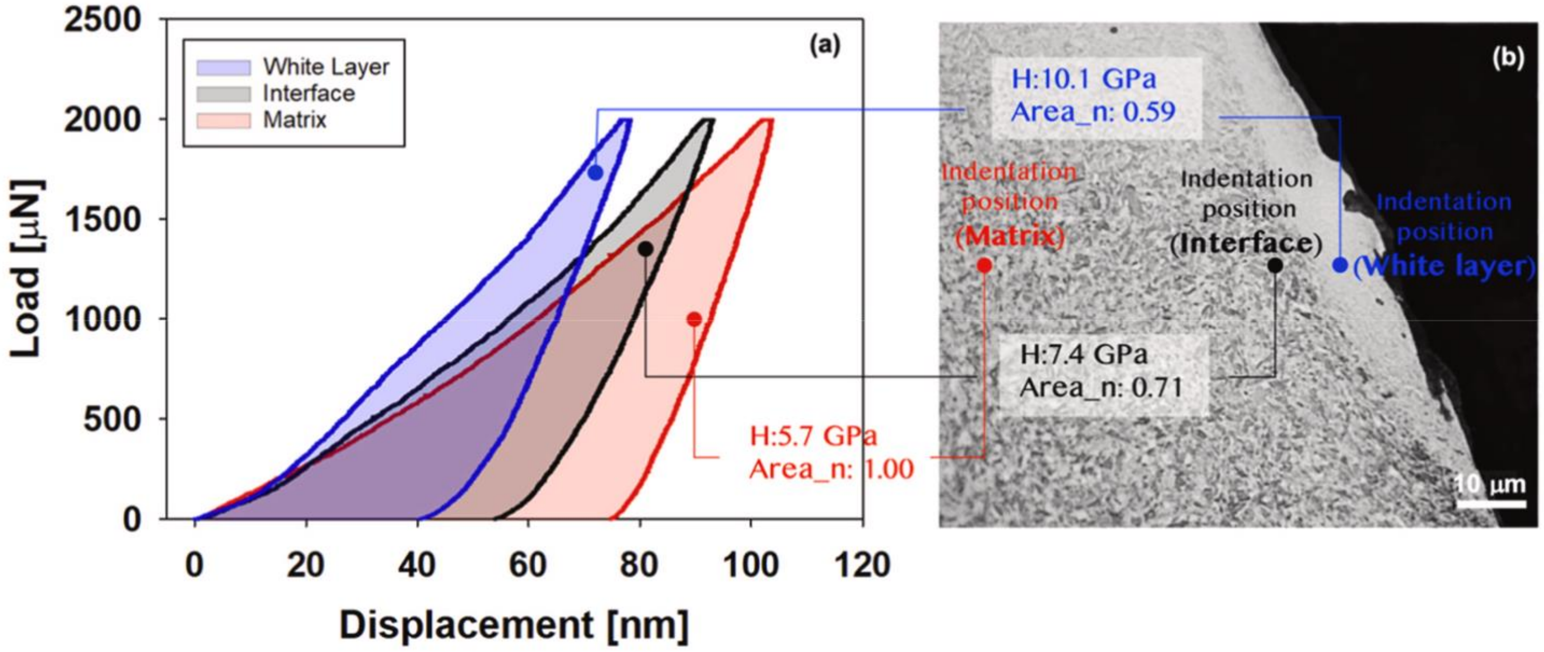

Fig. 14. a) The displacement-load curves of WL, bulk material, and interface region along with b) the hardness value, the ratio of area under each curve to the area under bulk material curve (Area _n) and position of each measurement.

Conclusion

- The model should be improved to be able to help formulating a balance between WL formation and destruction in favour of improving the erosion performance by including the **crystal plasticity, work hardening** effect as well as considering the **multi-directional impacts** in order to reach the optimum process parameters, especially **particle size & velocity.**

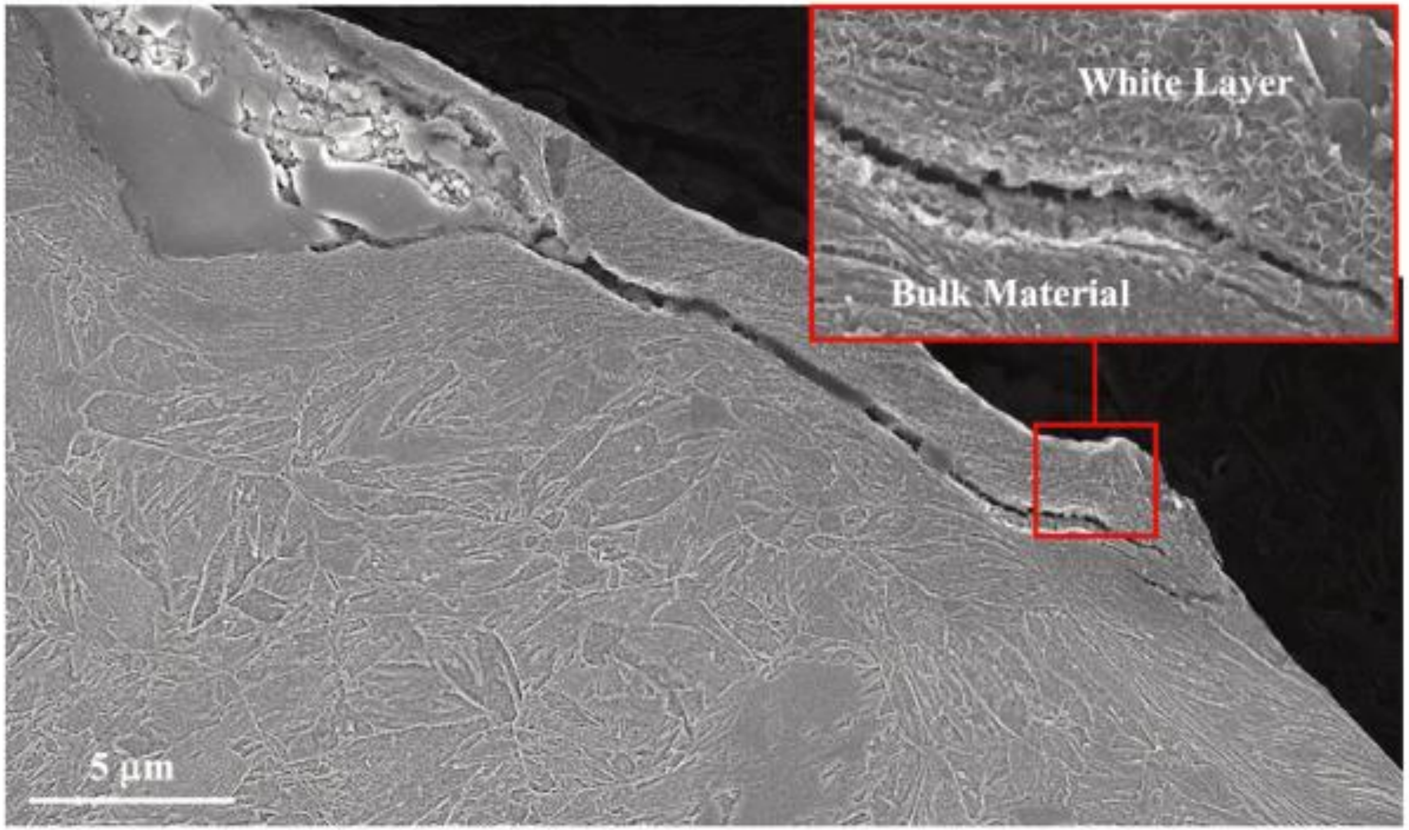

Fig. 17. An example of the cross-section of the surface damaged. Crack is initiated by an embedded particle and then propagated along the interface of the WL and bulk material (FESEM image).

Thanks for your attention

Welcome to ask !